Original Article

NOTCH4 Is a New Player in the Development of Pulmonary Fibrosis

Nadezhda Bakalenko[1]* , Daria Smirnova[1], Liana Gaifullina[1], Polina Kuchur[1], Daniela Ian[1],
Mikhail Atyukov[2], Ju Liu[3] and Anna Malashicheva[1]

[1]*Institute of Cytology, Russian Academy of Sciences, St-Petersburg, Russia;* [2]*St.Petersburg State Budgetary Institution of Health Care "City Multidisciplinary Hospital No. 2", St-Petersburg, Russia;* [3]*Institute of Microvascular Medicine, Medical Research Center, The First Affiliated Hospital of Shandong First Medical University and Shandong Provincial Qianfoshan Hospital, Jinan, China*

Abstract

Background and objectives: Idiopathic pulmonary fibrosis is a chronic, progressive, incurable lung disease, leading to irreversible lung tissue remodeling. The Notch signaling pathway, essential for lung development, has gained attention for its role in pulmonary fibrosis. While *Notch1* and *Notch3* have been extensively studied, the involvement of other Notch receptors, especially *Notch4*, remains less explored. This study aimed to evaluate the impact of *Notch4* on lung fibroblast activation and its potential interaction with the transforming growth factor-beta 1 (TGFβ1) signaling.

Methods: Primary human lung fibroblasts were transduced with lentivirus containing the intracellular domain of NOTCH4 (N4ICD). Changes in gene expression in transduced cells were assessed using real-time polymerase chain reaction, immunofluorescence staining, and Western blotting. Transcriptomic analysis was also performed on N4ICD-transduced lung fibroblasts.

Results: N4ICD overexpression significantly upregulated key fibrotic markers such as *ACTA2* and *COL1A1*. It also induced the TGFβ1 pathway, as evidenced by SMAD2 phosphorylation and elevated *TGFβ1* mRNA level. Transcriptomic analysis revealed that N4ICD-induced cells exhibited characteristics of highly invasive myofibroblasts.

Conclusions: This study establishes *Notch4* as a novel contributor to pulmonary fibrosis, by demonstrating its ability to induce myofibroblast differentiation and interact with the TGFβ1 pathway.

Introduction

Idiopathic pulmonary fibrosis (IPF) is a progressive condition characterized by excessive proliferation of connective tissue and abnormal deposition of the extracellular matrix (ECM), leading to irreversible remodeling of lung tissue and impaired respiratory function. The prevalence of fibrotic lung disorders such as IPF is increasing driven by the unprecedented aging of the global population.[1] The incidence of pulmonary fibrosis has also risen due to the COVID-19 pandemic. Without treatment, 50% of IPF patients die within three years of diagnosis, though treatment can extend life expectancy to seven to eight years.[2]

An essential factor in the development of fibrosis is the accumulation of myofibroblasts in lung tissues. Myofibroblasts synthesize large amounts of ECM and produce fibrogenic cytokines.[3] The cellular sources of myofibroblasts in lung fibrosis are not fully established. Various studies have shown that myofibroblasts may originate from lung stromal cells, including resident fibroblasts and pericytes, from mesenchymal stem cells in the bone marrow, and through the transdifferentiation of alveolar epithelial cells.[4]

The molecular mechanisms leading to myofibroblast differentiation remain incompletely understood, but transforming growth factor-beta 1 *(TGFβ1)* plays a significant role in these processes.[5,6] Fibrotic tissue transformation includes the epithelial-to-mesenchymal transition (EMT), and *TGFβ1* is crucial in triggering EMT during fibrotic processes in multiple tissues, including the lungs.[7]

The Notch signaling pathway plays a crucial role in lung development, particularly in regulating epithelial-mesenchymal interactions during alveologenesis, and contributes to maintaining the integrity of the epithelial and smooth muscle layers of de-

veloping distal airways. Many components of the Notch signaling pathway are activated in adults with various lung diseases.[8] In recent decades, accumulating data have shed light on the role of the Notch signaling pathway in the development of pulmonary fibrosis.[3,4,9–11] In mammals, four receptors of the Notch signaling pathway (*Notch1-4*) have been described. To date, their involvement in fibrosis development has been studied to varying degrees. The activation of *Notch1* leads to myofibroblast differentiation in alveolar epithelial cells,[4] pericytes,[9] and murine lung fibroblasts.[3] Animal models of lung fibrosis have shown that the deficiency of *Notch1* or *Notch3* significantly reduces the number of myofibroblasts and largely prevents fibrotic changes in lung tissue.[10,11] The involvement of *NOTCH2* in pulmonary fibrosis is less studied, but this receptor can also promote fibrogenetic changes in lung fibroblasts.[12] There is scarce data regarding the role of Notch4 in the development of fibrosis.

The interaction between the Notch and TGFβ signaling pathways in fibrosis is poorly understood. It showed that *Notch1* induces the expression of *TGFβ1* and phosphorylation of SMAD family member 3 (SMAD3) in rat alveolar epithelial cells. The induced expression of *Acta2* by TGFβ1 is partially mediated by Notch signaling.[4] Moreover, there is evidence that Notch signaling mediates TGFβ1-induced EMT in alveolar epithelial cells (A549) through the direct modulation of *Snai1*.[13] Notch inhibitor suppressed proliferation and migration of TGFβ1-treated human urethral scar fibroblasts.[14]

Earlier, we demonstrated that the overexpression of intracellular domains of all four *Notch* receptors (N1-4ICD) in primary cultures of human lung fibroblasts leads to the upregulation of *ACTA2 (α-SMA),* the most common molecular marker for myofibroblast differentiation. Surprisingly, the most prominent changes were observed in cells transfected with the intracellular domain of *NOTCH4* (N4ICD).[15] Until now, the involvement of *NOTCH4* in the progression of pulmonary fibrosis had not been established. In the present study, we demonstrated that the activation of the intracellular domain of the *NOTCH4* receptor induces the expression of myofibroblast and fibrotic markers in primary lung fibroblasts, and the pro-fibrotic effect of N4ICD transduction is partly mediated by the TGFβ pathway. Our study for the first time identifies Notch4 as a potential contributor to pulmonary fibrosis, making it a potential target for developing future drug therapies against the disease.

Materials and methods

Human lung fibroblast isolation and culture

The study was conducted using primary human lung fibroblasts obtained from patients without systemic lung or bronchial diseases, through partial resection of lung tissue. Research protocols were approved by the local ethics committee of St. Petersburg City Healthcare Institution "City Multidisciplinary Hospital No. 2" and adhered to the principles of the Helsinki Declaration. Written informed consent for participation in the study and tissue biopsy was obtained from all patients. Four men with a diagnosis of primary spontaneous pneumothorax participated in the study. The patients' ages were 32, 33, 35, and 38 years. Lung tissue fragments were cut into smaller pieces, and washed with phosphate-buffered saline (PBS), and cell isolation was performed with 0.1% collagenase solution for 2 h at 37°C (collagenase type II, 100 u/μL, Worthington Biochemical Corporation, USA). Cell suspensions were centrifuged (300 g, 5 m, room temperature). The cell pellets were resuspended in Dulbecco's Modified Eagle Medium (DMEM) (Gibco, Thermo Fisher, Waltham, MA, USA) supplemented with 10% fetal calf serum (Hyclone Laboratories, Logan, UT), 50 units/mL penicillin, and 50 μg/mL streptomycin (Invitrogen, Carlsbad, CA, USA), and seeded into tissue culture grade sterile plastic T25 flasks (Corning Incorporated, Corning, NY, USA) coated with 0.1% gelatin solution. The remaining small pieces of lung tissue were washed twice in PBS and also placed in plastic Petri dishes (Corning Incorporated, Corning, NY, USA) coated with 0.1% gelatin solution. The dishes' surfaces were scratched to improve tissue attachment. The cells were incubated at 37°C in 5% CO2, with the culture medium changed every four days. On the 7th-10th day, lung fibroblasts were passaged. Subsequent cultivation was carried out in Human Lung Fibroblast Media (HLFM) (Cell Applications Inc, USA). The study was performed on lung fibroblasts of the second or third passage.

All experiments were conducted using 6-well culture plates. The cells were seeded at a density of 200×10^3 cells per well for experiments lasting 1–3 days. For transcriptomic analysis, RNA was isolated on the 8th day, so cells were seeded at a density of 65×10^3 cells per well.

For TGFβ1 treatment, we used TGFβ1 (HiMedia Laboratories Pvt Ltd, Maharashtra, India) at a concentration of 20 ng/mL. The TGFβ1-containing medium was changed every two days.

Genetic constructs and lentivirus production

The lentiviral packaging plasmids were kindly provided by Dr. Trono from the École Polytechnique Fédérale de Lausanne, Switzerland. Lentiviral production followed a previously described protocol.[16] Briefly, subconfluent 293T cells in 100-mm dishes were co-transfected with 15 μg of pLVTHM-T7, 5.27 μg of pMD2.G, and 9.73 μg of pCMV-dR8.74psPAX2 using a polyethylenimine reagent. The next day, the medium was replaced with fresh medium, and the cells were incubated for 24 h to achieve high-titer virus production. The lentivirus was then concentrated from the supernatant by ultracentrifugation, resuspended in 1% bovine serum albumin (BSA) in PBS, and frozen in aliquots at −80°C. The efficiency of transduction was determined using a GFP-expressing virus, and the transduction efficiency was 85–90% based on GFP expression. The lentiviruses carrying coding sequences of the NOTCH1 intracellular domain were previously described.[17]

Total RNA isolation and real-time polymerase chain reaction (RT-PCR) analysis

Total RNA from the cultured cells was isolated using ExtractRNA (Eurogen, Moscow, Russia). For reverse transcription, we used 1 μg of RNA and the MMLV RT kit (Eurogen, Moscow, Russia). RT-PCR was performed with 2.5 μL cDNA and SYBRGreen PCR Mastermix (Eurogen, Moscow, Russia) in the Light Cycler system using specific forward and reverse primers for the target genes. The thermocycling conditions were as follows: 95°C for 5 m, followed by 45 cycles of 95°C for 15 s and 60°C for 1 m. A final heating step from 65°C to 95°C was performed to obtain the melting curves of the final PCR products. Changes in target gene expression levels were calculated as fold differences using the comparative ddCT method. The messenger RNA (mRNA) levels were normalized to glyceraldehyde 3-phosphate dehydrogenase (GAPDH) mRNA.

Western blotting

Protein was isolated using RIPA Buffer (ThermoFisher, 89901) supplemented with protease inhibitors (Roche, 11836170001). Proteins were subjected to 10% sodium dodecyl sulfate-polyacrylamide gel electrophoresis (SDS-PAGE) and then transferred

onto a 0.45 µm nitrocellulose membrane (Bio-Rad, 1620115). Following the transfer, membranes were blocked in PBS containing 5% non-fat dry milk and TBS containing 5% bovine serum albumin and incubated overnight at 4°C with primary antibodies diluted in blocking buffer (1:1,000): Smad2 (Cell Signaling Technology, D43B4, 5339), pSmad2 (Cell Signaling Technology, 134D4, 3108L), and β-actin (Cell Signaling Technology, 13E5, 4970). Membranes were then incubated for 1 h at ambient temperature with a goat anti-rabbit IgG HRP-linked secondary antibody (Invitrogen, 65-6120) diluted in blocking buffer (1:3,000). Blots were developed using SuperSignal West Femto Maximum Sensitivity Substrate (ThermoFisher, 34096) and SuperSignal West Pico PLUS Chemiluminescent Substrate (ThermoFisher, 34580). Images were acquired with a ChemiDoc MP Imaging System (Bio-Rad, USA). Three independent Western blots were used for each protein quantification.

Statistical analysis

Values are expressed as means ± SD. Groups were compared using the Mann–Whitney non-parametric test. A value of $p \leq 0.05$ was considered significant. Statistical analysis was performed using GraphPad Prism software (version 8.0.1, GraphPad Software, Boston, Massachusetts, USA).

Immunocytochemical staining

Cells were cultured on coverslips and fixed for 30 m in 4% paraformaldehyde at room temperature. Following fixation, fibroblasts were permeabilized with a 0.1% Triton X-100 solution for 10 m, washed with PBS, and blocked in 1% BSA for 1 h. Cell incubation with primary antibodies against α-SMA (ACTA2) (1:250, NB300-978, Novus, USA) or SNAIL (1:250, MA5-14801, Invitrogen, USA) was performed in a humid chamber for 1 h at room temperature. Subsequently, cells were washed three times with PBS for 5 m and incubated with secondary antibodies conjugated with Alexa546 or Alexa488 (Invitrogen, USA). Coverslips with cells were washed three times in PBS and mounted using Ibidi mounting medium with 4′,6-diamidino-2-phenylindole (DAPI) (Ibidi GmbH, Germany). Visualization and analysis were conducted with a confocal microscope Olympus FV3000 (Olympus Corporation, Japan) at 40× magnification and corresponding software.

Transcriptome analysis

For transcriptome analysis, RNA samples were prepared from primary cultures of lung fibroblasts obtained from three patients. For each patient, RNA was isolated from cells transduced with the control vector pCIG and cells transduced with a vector carrying the N4ICD on the 8th day after transduction.

The assessment of read quality was performed using FastQC v0.12.1 and MultiQC v1.14. Sequencing data underwent adapter trimming via Trimmomatic v0.39. The processed reads were subsequently aligned to the indexed human genome (NCBI accession number GCF_000001405.40) using the STAR v2.7.10b tool. Following alignment, transcript quantification for each annotated gene was conducted using featureCounts v2.0.3. Differential gene expression analysis was carried out using the DESeq2 tool following the standard algorithm. During data processing, genes with low read coverage (threshold = 10) were removed. The samples of rlog-transformed data were clustered by principal component analysis (PCA) and sparse partial least squares discriminant analysis (sPLS-DA) from the MixOmics library. sPLS-DA was used in addition to PCA as a more sensitive method. Based on the identified differentially expressed genes, functional annotation, and pathway enrichment analysis were performed using the clusterProfiler package and the Reactome Pathway database. The outcomes of the differential gene expression analysis were visually represented using ggplot2, EnhancedVolcano, and ComplexHeatmap.

Statistical transcriptomic data analysis

We conducted statistical data analysis on cells transduced with a vector carrying N4ICD in comparison to cells transduced with the control vector pCIG. The null hypothesis posits the lack of differential expression between the N4ICD and pCIG groups (log Fold Change = 0). The Wald test was employed to assess this hypothesis. This test was done as a component of the standard DESeq2 analysis used for comparing two groups.

Results

N4ICD induced the expression of genes associated with myofibroblast differentiation

To examine the effect of *NOTCH4* receptor activation in our primary lung fibroblast cultures, we ectopically expressed the N4ICD using lentivirus. The expression efficiency of N4ICD transduction is shown in Figure 1a. On the third day after N4ICD transduction, morphological changes were observed: N4ICD-infected cells appeared wider and less elongated compared to untreated cells or cells infected with control lentivirus (Fig. 1b). RT-PCR analysis showed that mRNA levels of EMT-associated genes *SNAI1* and *SNAI2* increased in N4ICD-transduced cells relative to pCIG-transduced cells. *SNAI1* mRNA level increased approximately 35-fold, and *SNAI2* expression grew 2.5-7-fold. We also observed a significant increase in the expression levels of genes relevant to myofibroblast differentiation, including collagen I (*COL1A1*) and the most common molecular marker for myofibroblasts ACTA*2* (α-SMA) (Fig. 1c). *ACTA2* and *COL1A1* mRNA levels increased more than 100-fold. The considerable variation in values seems to be attributed to the individual characteristics of the patients from whom the lung fibroblast cultures were derived. Immunofluorescence staining on day 3 after lentiviral transduction showed that SNAI1 was expressed much more strongly in N4ICD-transfected fibroblasts than in control cells or pCIG-transfected cells (Fig. 1d). As shown in Figure 1e, ACTA2 was also strongly positive and formed a prominent cytoskeleton in N4ICD–transduced cells. In untreated and pCIG-transduced fibroblasts, filamentous structures of ACTA2 were not detected. All these changes strongly indicate the induction of fibrosis in lung fibroblast cultures transduced with N4ICD-bearing lentivirus.

N4ICD-induced activation of the TGFβ1 pathway

Western blot analysis showed that overexpression of N4ICD induced phosphorylation of SMAD2, indicating the activation of the TGFβ pathway (Fig. 2a, Fig. S1). RT-PCR revealed that N4ICD upregulated the mRNA expression of *TGFβ1* and its receptor *TGFBR1* (Fig. 2b). Notably, N4ICD caused a more prominent increase in *TGFβ1* and *TGFBR1* expression than *TGFβ1* itself.

N4ICD promoted more intensive fibrogenesis than TGFβ1

We incubated lung fibroblasts with *TGFβ1* for three days and then assessed changes in the expression levels of EMT-associated genes *SNAI1* and *SNAI2* and genes of myofibroblast differentiation *ACTA2* and *COL1A1*. The mRNA concentration of all these genes exhibited an increase (Fig. 2c), but this upregulation was not as dramatic as in N4ICD-transduced fibroblasts, especially for
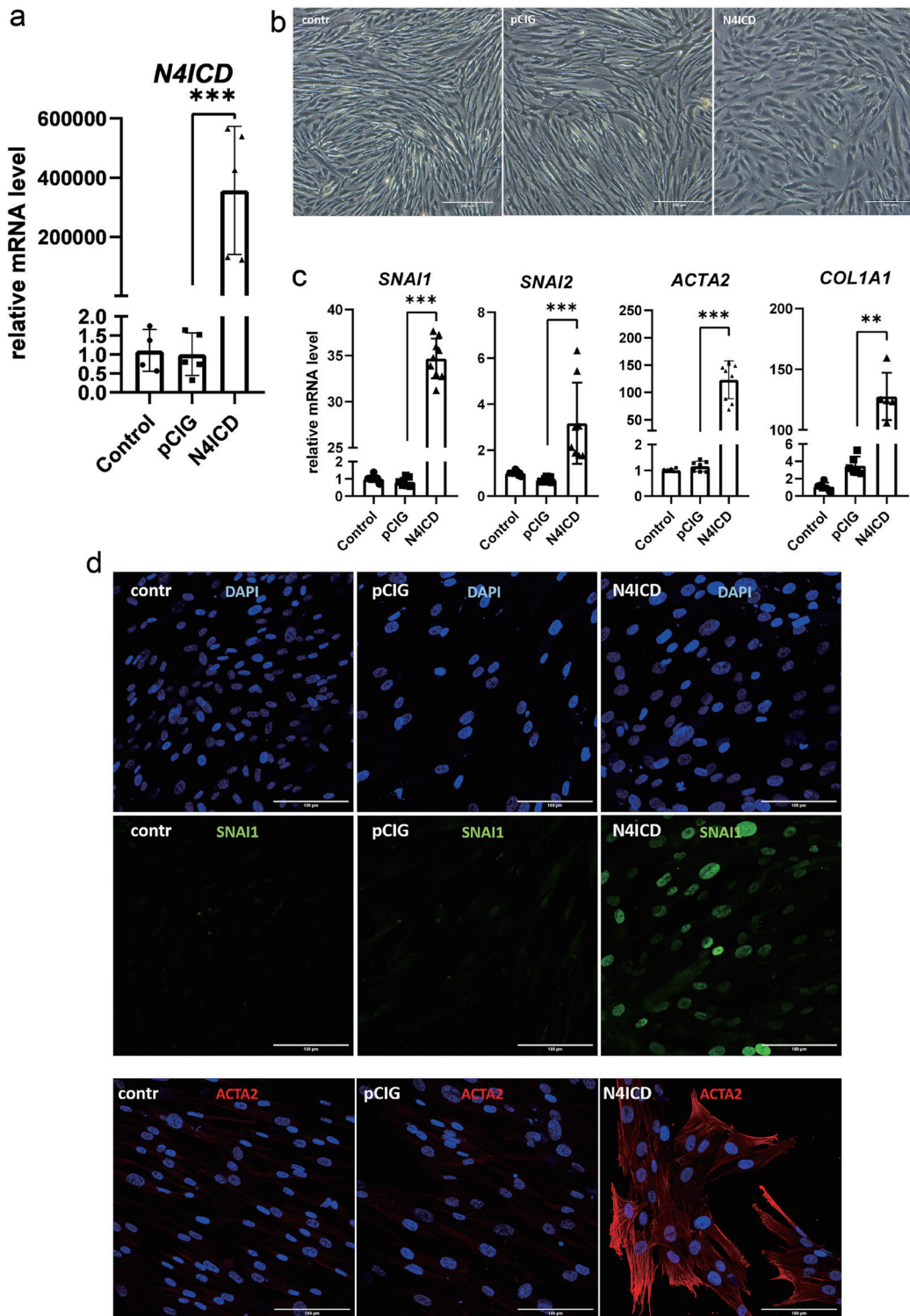
Fig. 1. Induction of fibrogenesis-associated genes in human lung fibroblasts on day 3 after N4ICD transduction. contr – untransduced fibroblasts; pCIG – control vector transduced fibroblasts; N4ICD – N4ICD-transduced fibroblasts. (a) Expression efficiency of N4ICD transduction was evaluated by RT-PCR analysis with primers for N4ICD. *** $p < 0.001$. (b) Morphological changes in N4ICD-transduced cells compared to control ones. (c) RT-PCR results for *SNAI1, SNAI2, ACTA2,* and *COL1A1* in control, pCIG- and N4ICD-transduced cells. *** $p < 0.001$; ** $p < 0.01$. (d) and (e). Immunofluorescence labeling analysis of control, pCIG- and N4ICD-transduced cells. Nuclei were stained with DAPI (blue). (d) Immunofluorescence staining with SNAI1 antibodies (green). (e) Immunofluorescence staining with ACTA2 antibodies (red). DAPI, 4′,6-diamidino-2-phenylindole; mRNA, messenger RNA; N4ICD, NOTCH4 intracellular domain; RT-PCR, real-time polymerase chain reaction.
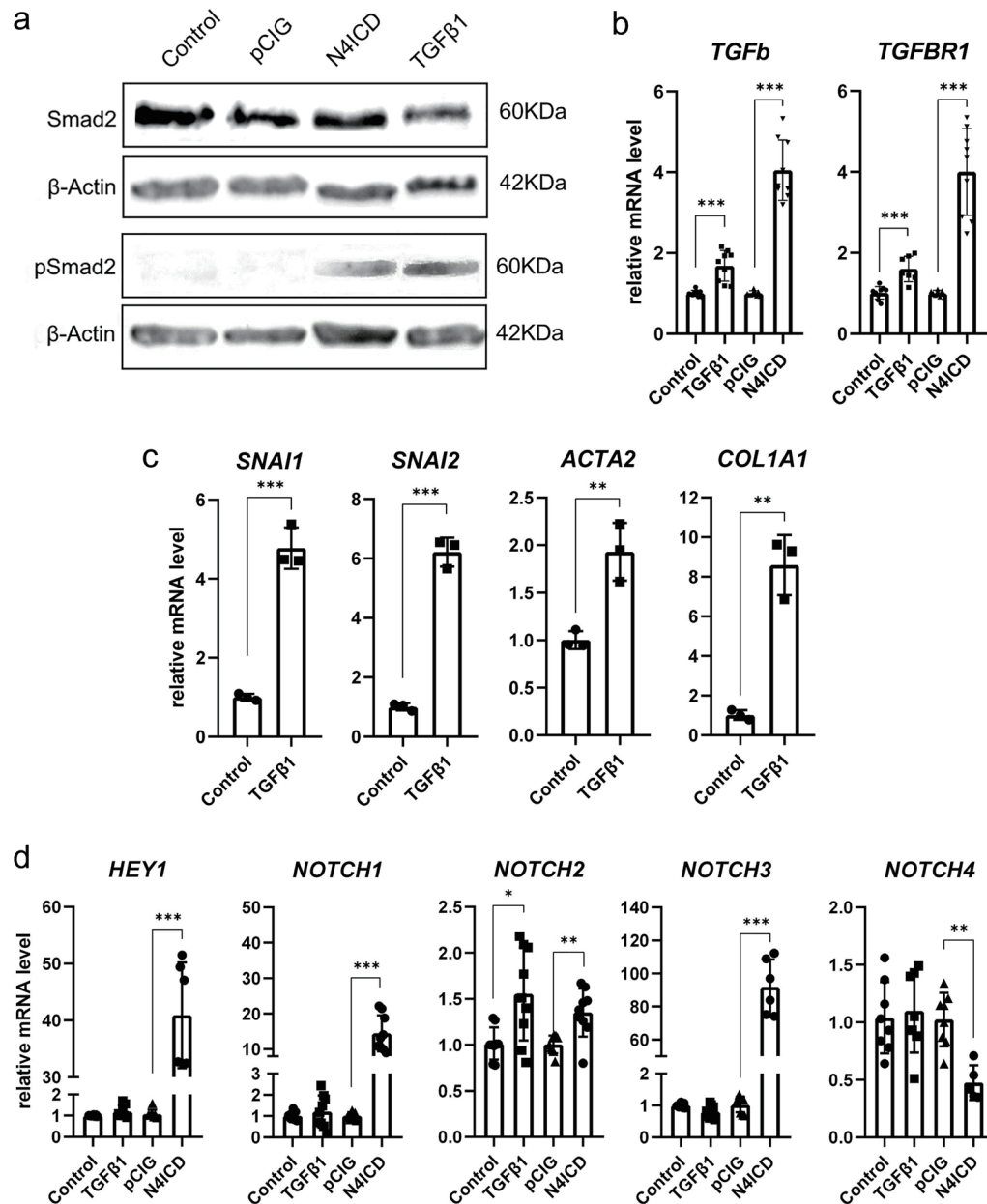
Fig. 2. The reciprocal impact of Notch4 and TGFβ1 pathways on each other. Control – untreated fibroblasts; pCIG – control vector transduced fibroblasts; N4ICD – N4ICD-transduced fibroblasts, TGFβ1 – treated lung fibroblasts. (a) Western blot analysis of control, pCIG- and N4ICD-transduced and TGFβ1 – treated fibroblast after 48 h after treatment. Membranes were incubated with Smad2, phosphorylated SMAD2 (pSmad), and b-actin antibodies. (b)-(d) Gene expression evaluation in TGFβ1-treated or N4ICD-induced lung fibroblasts on day 3 by RT-PCR. Expression in TGFβ1-treated cells is shown relative to control cells; expression in N4ICD-induced cells is shown relative to pCIG-transduced cells. *** $p < 0.001$; ** $p < 0.01$; * $p < 0.05$. (b) *TGFβ1* and *TGFBR1* expression in TGFβ1-treated or N4ICD-induced lung fibroblasts. (c) Fibrogenesis-associated genes *SNAI1, SNAI2, ACTA2,* and *COL1A1* expression in TGFβ1-treated lung fibroblasts. (d) *HEY1, NOTCH1, NOTCH2, NOTCH3, NOTCH4* expression in TGFβ1-treated or N4ICD-induced lung fibroblasts. N4ICD, Notch4 intracellular domain; RT-PCR, real-time polymerase chain reaction; SMAD2, smad family member 2; TGFβ1, transforming growth factor beta 1.

ACTA2 and collagen I (Figs. 2c vs Fig. 1c). Therefore, we cannot explain the strong profibrotic effect of N4ICD transduction by the induction of the TGFβ1 pathway alone.

The impact of TGFβ1 and N4ICD on Notch pathway components

According to RT-PCR data, incubation with TGFβ1 does not lead to noticeable changes in the expression levels of *NOTCH1, NOTCH3,* and *NOTCH4* receptors or the *NOTCH* signaling target *HEY1,* but causes a slight increase in *NOTCH2* expression. In contrast, N4ICD significantly enhances the expression of mRNA for *HEY1, NOTCH1,* and *NOTCH3,* with no significant changes detected in the expression levels of *NOTCH2.* Remarkably, *NOTCH4* expression decreased slightly in N4ICD-transduced fibroblasts (Fig. 2d).
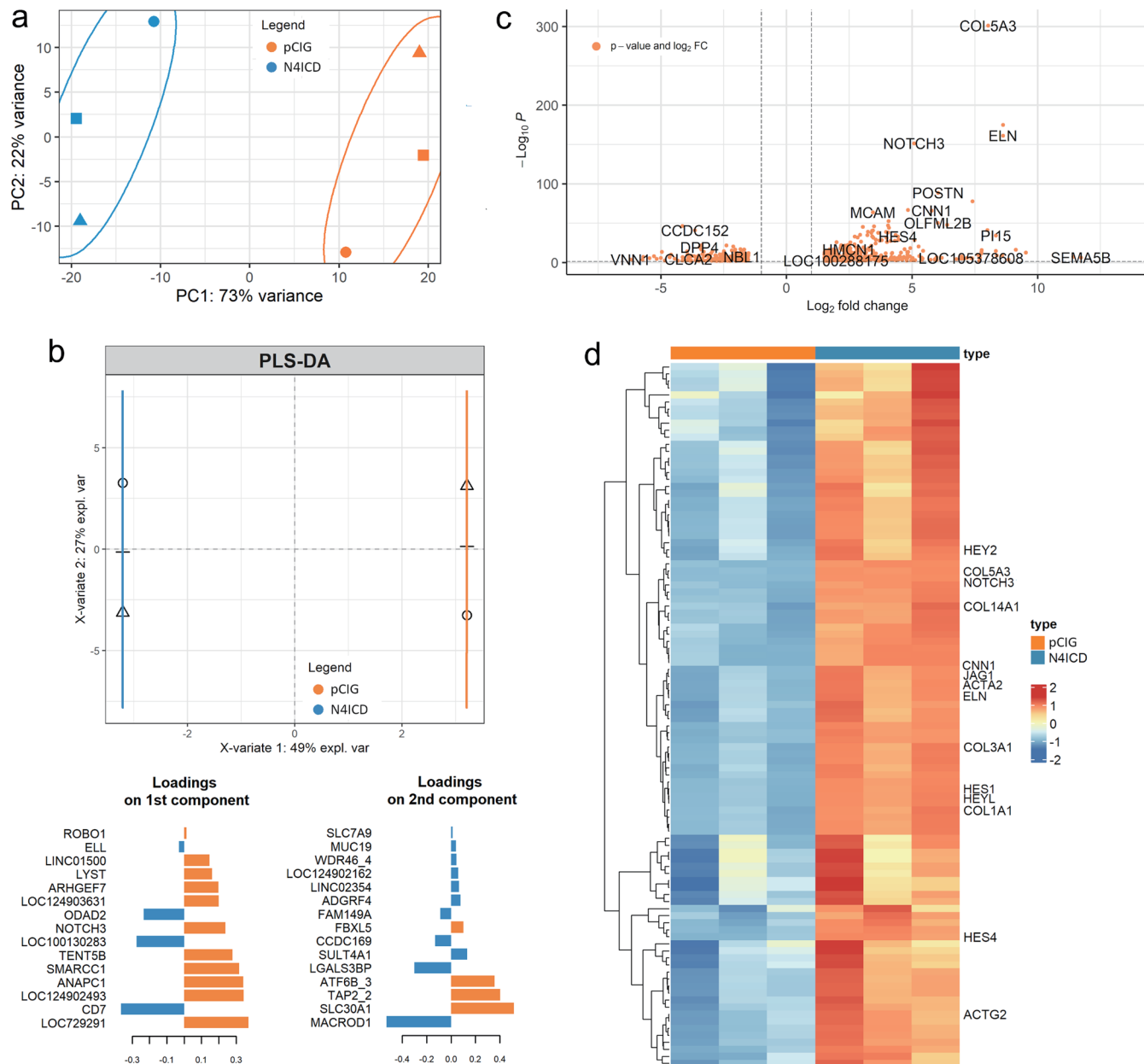
Fig. 3. Transcriptomic analysis of lung fibroblasts with the activated intracellular domain of the NOTCH4 receptor (N4ICD) in comparison with the control (pCIG). Clustering of samples in (a) PCA dimension, and (b) sPLS-DA based on transcriptomic data. Blue – N4ICD-activated samples; Orange – control group (pCIG) samples. (c) Volcano plot showing the log10 dependency on the log2 fold change of significantly upregulated or downregulated genes in N4ICD-activated samples compared to pCIG. Genes with a logarithmic fold change greater than 1.5 and a p-value less than 0.05 are denoted in orange. (d) Heatmap of the top 100 differentially expressed genes between the N4ICD (blue) and pCIG (orange) sample clusters. N4ICD, Notch4 intracellular domain; PCA, principal component analysis; sPLS-DA, sparse partial least squares discriminant analysis.

Transcriptomic analysis of lung fibroblasts transduced with a N4ICD

The identification of differentially expressed genes (DEGs) was conducted by comparing the RNA sequencing data from samples with activated N4ICD and control samples pCIG. DEGs were selected based on the following threshold values: |logFC| > 1.5 and adjusted *p*-value < 0.05. According to PCA and sPLS-DA, the samples formed two clusters - pCIG and N4ICD (Fig. 3a, b).

In the samples with activated N4ICD, 640 DEGs were identified, with 413 exhibiting positive regulation and 227 showing negative regulation, indicative of significant changes in the transcriptional landscape. Among the DEGs, genes serving as targets of Notch signaling, including *HEYL* (logFC = 9.13, p.adj = 1.28e-11), *HES1* (logFC = 6.39, p.adj = 2.43e-45), *HES4* (logFC = 4.44, p.adj = 4.61e-31), and the upregulation of the *NOTCH3* gene (logFC = 5.07, p.adj = 1.39e-148) (Fig. 3c, d) were present, confirming the activation of Notch signaling in N4ICD samples.

Table 1. Genes encoding collagens activated in N4ICD-transduced cells

Collagens	N4ICD vs pCIG (logFC)
COL5A3	8.03
COL14A1	5.29
COL3A1	4.29
COL1A1	4.04
COL5A1	3.41
COL3A1_1	3.27
COL4A2	3.24
COL18A1_1	2.54
COL5A2	2.54
COL1A2	2.33
COL4A6	−2.21
COL6A3	1.72
COL6A1	1.67

N4ICD, Notch4 intracellular domain.

Significantly, in N4ICD-induced samples, there is an upregulation in the expression of genes associated with fibrosis (*ELN*, logFC = 8.62, p.adj = 2.83e-158; *COL1A1*, logFC = 4.04, p.adj = 7.10e-45; *ACTA2*, logFC = 3.96 p.adj = 1.06e-36) and collagen synthesis (Table 1, Fig. 3c, d). Additionally, several genes are identified as markers of myofibroblasts (*WNT5A*, logFC = 2.36, p.adj = 8.40e-11; *ACTG2*, logFC = 4.31, p.adj = 8.86e-26; *CNN1*, logFC = 5.78, p.adj = 2.14e-63), particularly those marking early myofibroblasts (*ACTA2*, logFC =3.96, p.adj = 1.06e-36; *TAGLN*, logFC = 1.91, p.adj = 2.47e-9).[18] Alongside fibrotic markers, genes related to TGFβ signaling, which mediate cell differentiation into myofibroblasts, were identified (*TGFβ3*, logFC = 2.70, p.adj = 3.14e-9; *TGFβ2*, logFC = 1.44, p.adj = 0.0001; *TGFβ1*, logFC = 1.37, p.adj = 1.73e-9; *SKIL*, logFC = 1.87, p.adj = 1.88e-5; *INHBA*, logFC = 3.87, p.adj = 0.0008; *SERPINE1*, logFC = 1.59, p.adj = 1.66e-9). Lastly, the RhoA pathway was examined, specifically noting the expression level of the *SFRP1* gene (logFC = −2.39, p.adj = 4.99e-20), known to suppress myofibroblast invasiveness.[19]

Enrichment analysis of the biological processes ontology reveals that positively regulated DEGs are involved in regulating Notch signaling, ECM metabolism, and collagen fibril assembly (Fig. 4a). The correlation of DEGs with relevant pathways according to the Reactome Pathway database aligns with the ontology-based analysis, revealing enrichment in pathways such as ECM organization, collagen biosynthesis and formation, and assembly of collagen fibrils (Fig. 4b).

Based on the identified DEGs, it can be inferred that the investigated cells exhibit the phenotype of highly invasive myofibroblasts. Typically, these cells appear during trauma to regenerate
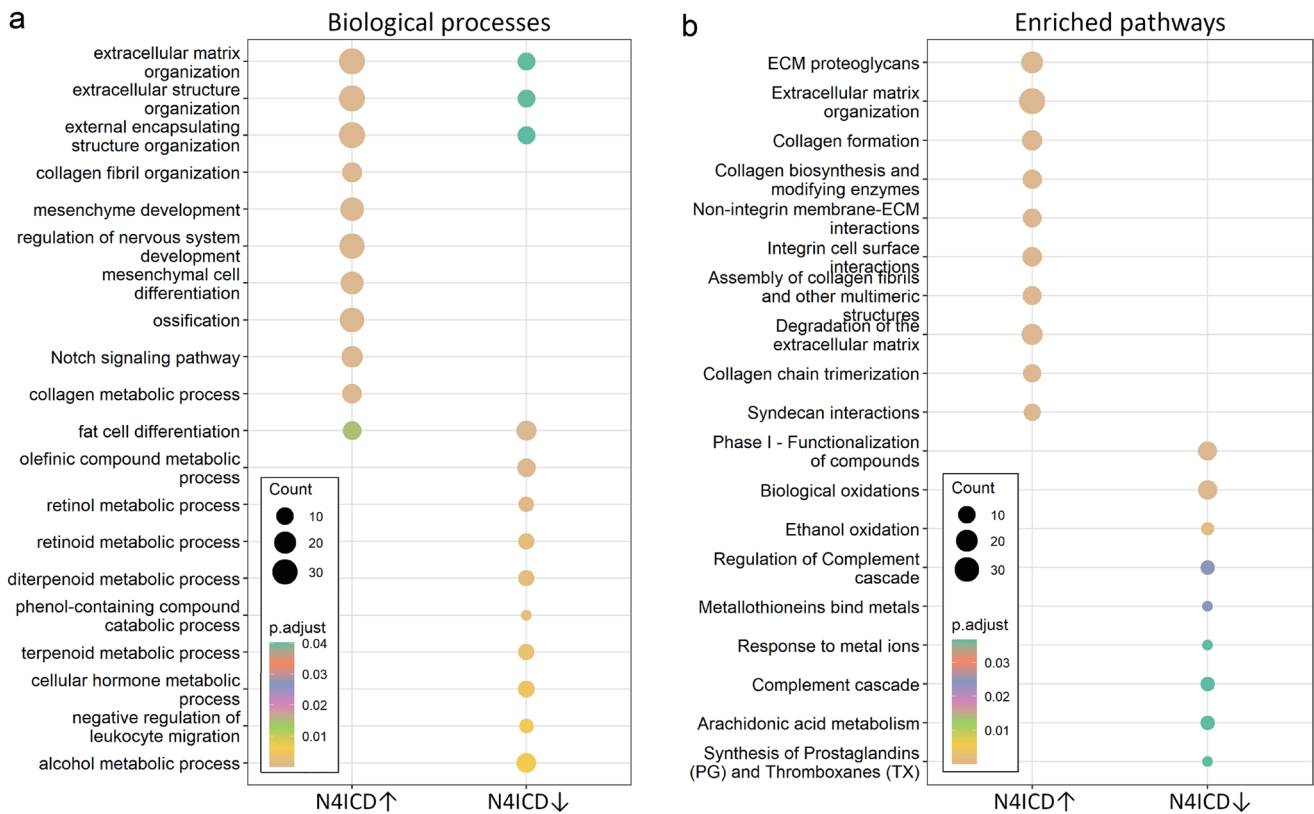

Fig. 4. Enrichment analysis of differentially expressed genes that are upregulated (N4ICD↑) or downregulated (N4ICD↓) in lung fibroblasts with activated N4ICD, as compared to the control samples pCIG, conducted using (a) the "Biological Processes" Gene Ontology and (b) pathways according to the Reactome Pathway database. The selection of DEGs is based on logarithmic fold change (greater than 1.5) and adjusted p-value (less than 0.05) thresholds. DEGs, differentially expressed genes; N4ICD, Notch4 intracellular domain.

damaged tissues. However, in fibrosis, they accumulate, leading to increased production of ECM.

Discussion

Numerous studies in recent years have confirmed the involvement of Notch signaling in the development of fibrosis in various organs and tissues. However, the majority of these studies have focused on the role of *NOTCH1* in fibrogenesis. Nevertheless, other Notch receptors may be equally significant in these pathological processes. Among these, *NOTCH4* is the least explored. It is known that its expression increases during liver fibrogenesis,[20] and that it is crucial for shear-mediated renal fibrosis.[21] Our research provides evidence that *NOTCH4* is capable of inducing significant upregulation of myofibroblast- and fibrosis-associated genes *in vitro* human pulmonary fibroblast cultures. Transcriptomic analysis revealed that on day 8 after N4ICD transduction, primary lung fibroblasts became highly invasive myofibroblasts.

We provide evidence that the *NOTCH4* signal acts upstream of the TGFβ1 pathway. RT-PCR data showed that N4ICD increased the production of *TGFβ1* mRNA. Transcriptomic data indicated upregulation of *TGFβ1, TGFβ2*, and *TGFβ3* in N4ICD-transduced cells. In addition, our Western blot analysis showed that *NOTCH4* induces the phosphorylation of SMAD2. Similar results were obtained in the rat alveolar epithelial cell line RLE-6TN, where *Notch1* activation enhanced *TGFβ1* expression and led to SMAD3 phosphorylation.[4] However, there is also evidence that *NOTCH4* promotes the degradation of phosphorylated SMAD3 and negatively regulates the protein level of *TGFβ1* itself.[21] It was also shown that in RLE-6TN cells, TGFβ1 upregulated the expression level of *Notch1*.[4] In the human lung fibroblast cell culture IMR-90, TGFβ1 treatment induced the expression of the *NOTCH3* receptor, but not *NOTCH1*.[22] According to our results, the impact of TGFβ1 on Notch expression in primary lung fibroblasts is barely detectable, indicating a high specificity of TGFβ1's impact in different cellular contexts.

TGFβ signaling is known as a powerful inductor of pulmonary fibrosis,[23] and we can assume that in primary lung fibroblasts, the TGFβ1 pathway can partially mediate the pro-fibrotic effect of N4ICD transduction. In these cells, the influence of N4ICD on myofibroblast differentiation was considerably more notable than the impact of incubation with TGFβ1, suggesting that N4ICD also has a TGFβ1-independent pathway to induce fibrogenesis. The transduction of N4ICD led to robust activation of *NOTCH3*. In the study by Vera and colleagues,[11] it was convincingly demonstrated that *NOTCH3* plays a substantial role in fibroblast activation and pulmonary fibrosis. It is possible that the strong induction of fibrogenesis by N4ICD is partly attributed to the activation of the Notch3 signaling pathway.

Conclusions

The limitation of the present study is that it was performed on cells obtained from a small number of donors and used *in vitro* cell culture models, which may not fully represent the complex *in vivo* environment of pulmonary fibrosis. Nevertheless, this study demonstrates that activation of the intracellular domain of the *NOTCH4* receptor is capable of initiating the differentiation of pulmonary fibroblasts into myofibroblasts. This finding establishes *NOTCH4* as a potential new player in the development of pulmonary fibrosis. To further investigate the role of *NOTCH4* in lung fibrogenesis, it is important to investigate its expression in

lung cells from patients with idiopathic pulmonary fibrosis. While N4ICD transduction has some influence on the TGFβ1 pathway, the interaction between the Notch and TGFβ1 signaling pathways in the regulation of fibrogenesis requires further research.

Conflict of interest

The authors declare no conflict of interests.

Author contributions

Study concept and design (AM, NB), acquisition of data (DS, LG, NB, MA, DI), analysis and interpretation of data (PK, NB, DS, JL), drafting of the manuscript (NB), critical revision of the manuscript for important intellectual content (NB, AM, JL), administrative, technical, or material support (AM, MA), and study supervision (AM). All authors have made a significant contribution to this study and have approved the final manuscript.

Ethics statement

Research protocols were approved by the local ethics committee of St. Petersburg City Healthcare Institution "City Multidisciplinary Hospital No. 2" and adhered to the principles of the Helsinki Declaration. Written informed consent for participation in the study and tissue biopsy was obtained from all patients.

Data sharing statement

The data that support the findings of this study are available from the corresponding author upon reasonable request.

References

[1] Raghu G, Chen SY, Hou Q, Yeh WS, Collard HR. Incidence and prevalence of idiopathic pulmonary fibrosis in US adults 18-64 years old. Eur Respir J 2016;48(1):179–186. doi:10.1183/13993003.01653-2015, PMID:27126689.

[2] Duong-Quy S, Vo-Pham-Minh T, Tran-Xuan Q, Huynh-Anh T, Vo-Van T, Vu-Tran-Thien Q, *et al*. Post-COVID-19 Pulmonary Fibrosis: Facts-Challenges and Futures: A Narrative Review. Pulm Ther 2023;9(3):295–307. doi:10.1007/s41030-023-00226-y, PMID:37209374.

[3] Liu T, Hu B, Choi YY, Chung M, Ullenbruch M, Yu H, *et al*. Notch1 signaling in FIZZ1 induction of myofibroblast differentiation. Am J Pathol 2009;174(5):1745–1755. doi:10.2353/ajpath.2009.080618, PMID:19349363.

[4] Aoyagi-Ikeda K, Maeno T, Matsui H, Ueno M, Hara K, Aoki Y, *et al*. Notch induces myofibroblast differentiation of alveolar epithelial cells via transforming growth factor-{beta}-Smad3 pathway. Am J Respir Cell Mol Biol 2011;45(1):136–144. doi:10.1165/rcmb.2010-0140oc, PMID:21749980.

[5] Kaarteenaho-Wiik R, Paakko P, Sormunen R. Ultrastructural fea-

tures of lung fibroblast differentiation into myofibroblasts. Ultra-struct Pathol 2009;33(1):6–15. doi:10.1080/01913120802608430, PMID:19191196.

[6] Bartram U, Speer CP. The role of transforming growth factor beta in lung development and disease. Chest 2004;125(2):754–765. doi:10.1378/chest.125.2.754, PMID:14769761.

[7] Willis BC, Borok Z. TGF-beta-induced EMT: mechanisms and implications for fibrotic lung disease. Am J Physiol Lung Cell Mol Physiol 2007;293(3):L525–L534. doi:10.1152/ajplung.00163.2007, PMID:17631612.

[8] Kiyokawa H, Morimoto M. Notch signaling in the mammalian respiratory system, specifically the trachea and lungs, in development, homeostasis, regeneration, and disease. Dev Growth Differ 2020;62(1):67–79. doi:10.1111/dgd.12628, PMID:31613406.

[9] Wang YC, Chen Q, Luo JM, Nie J, Meng QH, Shuai W, *et al*. Notch1 promotes the pericyte-myofibroblast transition in idiopathic pulmonary fibrosis through the PDGFR/ROCK1 signal pathway. Exp Mol Med 2019;51(3):1–11. doi:10.1038/s12276-019-0228-0, PMID:30902967.

[10] Hu B, Phan SH. Notch in fibrosis and as a target of anti-fibrotic therapy. Pharmacol Res 2016;108:57–64. doi:10.1016/j.phrs.2016.04.010, PMID:27107790.

[11] Vera L, Garcia-Olloqui P, Petri E, Viñado AC, Valera PS, Blasco-Iturri Z, *et al*. Notch3 Deficiency Attenuates Pulmonary Fibrosis and Impedes Lung-Function Decline. Am J Respir Cell Mol Biol 2021;64(4):465–476. doi:10.1165/rcmb.2020-0516OC, PMID:33493092.

[12] Liu P, Zhao L, Gu Y, Zhang M, Gao H, Meng Y. LncRNA SNHG16 promotes pulmonary fibrosis by targeting miR-455-3p to regulate the Notch2 pathway. Respir Res 2021;22(1):44. doi:10.1186/s12931-021-01632-z, PMID:33549106.

[13] Matsuno Y, Coelho AL, Jarai G, Westwick J, Hogaboam CM. Notch signaling mediates TGFβ1-induced epithelial-mesenchymal transition through the induction of Snai1. Int J Biochem Cell Biol 2012;44(5):776–789. doi:10.1016/j.biocel.2012.01.021, PMID:22330899.

[14] Huang S, Fu D, Wan Z, Li M, Li H, Chong T. Effects of a gamma-secretase inhibitor of notch signalling on transforming growth factor β1-induced urethral fibrosis. J Cell Mol Med 2021;25(18):8796–8808. doi:10.1111/jcmm.16837, PMID:34363303.

[15] Chistyakova IV, Bakalenko NI, Malashicheva AB, Atyukov MA, Petrov AS. [The role of Notch-dependent differentiation of resident fibroblasts in the development of pulmonary fibrosis]. Translational Medicine 2022;9(5):96–104. doi:10.18705/2311-4495-2022-9-5-96-104.

[16] Perepelina K, Klauzen P, Kostareva A, Malashicheva A. Tissue-Specific Influence of Lamin A Mutations on Notch Signaling and Osteogenic Phenotype of Primary Human Mesenchymal Cells. Cells 2019;8(3):266. doi:10.3390/cells8030266, PMID:30901896.

[17] Kostina AS, Uspensky VE, Irtyuga OB, Ignatieva EV, Freylikhman O, Gavriliuk ND, *et al*. Notch-dependent EMT is attenuated in patients with aortic aneurysm and bicuspid aortic valve. Biochim Biophys Acta 2016;1862(4):733–740. doi:10.1016/j.bbadis.2016.02.006, PMID:26876948.

[18] Liu X, Rowan SC, Liang J, Yao C, Huang G, Deng N, *et al*. Categorization of lung mesenchymal cells in development and fibrosis. iScience 2021;24(6):102551. doi:10.1016/j.isci.2021.102551, PMID:34151224.

[19] Mayr CH, Sengupta A, Asgharpour S, Ansari M, Pestoni JC, Ogar P, *et al*. Sfrp1 inhibits lung fibroblast invasion during transition to injury-induced myofibroblasts. Eur Respir J 2024;63(2):2301326. doi:10.1183/13993003.01326-2023, PMID:38212077.

[20] Gramantieri L, Giovannini C, Lanzi A, Chieco P, Ravaioli M, Venturi A, *et al*. Aberrant Notch3 and Notch4 expression in human hepatocellular carcinoma. Liver Int 2007;27(7):997–1007. doi:10.1111/j.1478-3231.2007.01544.x, PMID:17696940.

[21] Grabias BM, Konstantopoulos K. Notch4-dependent antagonism of canonical TGFβ1 signaling defines unique temporal fluctuations of SMAD3 activity in sheared proximal tubular epithelial cells. Am J Physiol Renal Physiol 2013;305(1):F123–F133. doi:10.1152/ajprenal.00594.2012, PMID:23576639.

[22] Lai JM, Zhang X, Liu FF, Yang R, Li SY, Zhu LB, *et al*. Redox-sensitive MAPK and Notch3 regulate fibroblast differentiation and activation: a dual role of ERK1/2. Oncotarget 2016;7(28):43731–43745. doi:10.18632/oncotarget.9667, PMID:27248323.

[23] Yue X, Shan B, Lasky JA. TGFβ: Titan of Lung Fibrogenesis. Curr Enzym Inhib 2010;6(2):67–77. doi:10.2174/157340810791233033, PMID:24187529.